

Article

Experimental Study on the Damage of Granite by Acoustic Emission after Cyclic Heating and Cooling with Circulating Water

Dong Zhu ^{1,2}, Hongwen Jing ^{1,*}, Qian Yin ¹ and Guansheng Han ¹

¹ State Key Laboratory for Geomechanics and Deep Underground Engineering, China University of Mining and Technology, Xuzhou 221116, China; zhudong163@163.com (D.Z.); jeryin@foxmail.com (Q.Y.); Han_GS@cumt.edu.cn (G.H.)

² College of Energy and Transportation Engineering, Jiangsu Vocational Institute of Architectural Technology, Xuzhou 221116, China

* Correspondence: hwjingcumt@126.com

Received: 27 June 2018; Accepted: 19 July 2018; Published: 25 July 2018



Abstract: Hot dry rock is developed by injecting cold water into high-temperature rock mass. At the same time, cold water is heated in contact with the rock mass. With the continuous influx of cold water, the surrounding rock will undergo a rapid cooling process, which results in several cycles of heating and cooling. However, there is little research on the influence of cycles of heating and cooling with circulating water on the mechanical properties of rock, which is of great importance to the stability of rock mass engineering in the process of energy development. In this paper, the effects of cyclic heating and cooling with circulating water on the damage of granite are studied using uniaxial compressive, Brazilian and acoustic emission (AE) tests. The results show that heat treatment temperature and number of cycles have important effects on the mechanical properties of granite as follows: (1) at the same treatment temperature, an increase in the number of cycles means that the distribution of physical and mechanical parameters of the granite show an almost exponential downward trend. The uniaxial compression of granite results in its transformation from brittle to plastic, and the failure mode changes from slipping of the shear surface to plastic failure. With increased cycles of heating and cooling with circulating water, the tensile strength of granite also decreases; temperature has an obvious influence on physical and mechanical parameters, cracking of samples, and plays a controlling role in the failure mode of samples. In addition, (2) at the same temperature, the heating and cooling numbers N have a significant influence on the AE distribution characteristics of the sample under uniaxial compression and the number of AE collisions, and the cumulative number of AE decreases with the increase of N . (3) The concepts of mechanical damage and high-temperature and cold-water shock damage during uniaxial compression of samples were proposed based on AE, and the damage equations were established respectively. The curve equations of damage value (D) and cycle numbers N after thermal shock damage of high temperature and cold water were overlaid. The cracking mechanism of high-temperature and cold water impact on granite was analyzed, and the thermal shock stress equation of high temperature and water cooling was established.

Keywords: damage; cyclic heating and cooling; physical and mechanical parameters; failure mode; acoustic emission

1. Introduction

With the increased development of geothermal resources and nuclear waste storage technology, seepage mechanics of fractured rock mass and high-temperature rock damage has become a hot research topic [1–7].

In previous literature, researchers have carried out work that examines the mechanical properties of rock after exposure to high temperatures, including the deformation process, failure criterion of rock under pressure, and thermal cracking, and provided constitutive equations and carried out rock damage characterization in response [8–13]. Many scholars have paid attention to the study of high-temperature rock damage [14–17]. Yu et al. [18] built a mesostructure based on the numerical model for the analysis of rock thermal cracking based on elastic damage mechanics and thermal-elastic theory. In addition, the damage accumulation induced by thermal (T) and mechanical (M) loads is considered to modify the elastic modulus, strength and thermal properties of individual elements in line with the intensity of damage. Yang et al. [19] across an experimental investigation on thermal damage and failure of mechanical behavior of granite after exposure to different high-temperature treatments, found that the internal damage mechanism of rock is obviously affected by temperature.

Acoustic emission (AE) technology is widely used in material damage monitoring and evaluation [20–26]. The AE patterns of rocks at different temperatures were studied under uniaxial compression and the relationship between rock damage and AE was established. Wu et al. [27] studied the relationship between microstructure morphology and AE of granite found: with increase of temperature, there was more internal crack formation and internal damage for granite, and more frequent AE activity of granite under uniaxial compression. The mechanical properties and AE characteristics of granite with the formation of internal crack networks of granite has a corresponding relationship. The peak stress curve and ringing cumulative number curve of granite have a stable trend when crack expansion is slow. However, the peak stress and the ringing cumulative number curve of granite will have inflection point and lead to mutation when the crack network expands rapidly. Chen et al. [28] used AE technology to evaluate the fracture strength and energy value of hard rock and concluded that AE and index increased with the increase of rock temperature. A study on the mechanical characteristics of high-temperature rocks after cooling is in the center of scientific research interests [29–34]. They studied the effects of different cooling rates and methods on mechanical parameters, strength cracking and failure modes of high-temperature rocks. Shao et al. [35] studied the effects of the cooling rate and the constituent grain size on the mechanical behavior of heated rock. They found that larger-grain granite rocks are more affected by water quenching, rocks that have been slowly cooled have areas with greater crack growth, and the stress threshold of medium-grain rocks that have been slowly cooled is affected.

However, studies on the mechanical properties and damage to granite during water cycle cooling have rarely been conducted. A laboratory experiment was designed in view of the current engineering application in drilling and underground space engineering fire rescues [36], especially for the study of rock mechanics in the process of dry hot rock development. In this study, the effects of the cycles of heating and cooling with circulating water on the physical and mechanical parameters, damage of granite and failure mode are studied by carrying out uniaxial compression, and Brazilian and AE tests. In addition, we established the damage equation of rock samples based on the characteristics of AE data.

2. Materials and Methods

2.1. Sample Collection and Preparation

The granite samples used in the experiment originated from Zhangzhou City in Fujian Province, China. These rocks are naturally gray and white in color, and compact and uniform with no voids or cracks on their surface. The main minerals determined by X-ray diffraction are feldspar 35%, quartz 40%, amphibole 20% and mica 5%. The initial moisture content of the sample is 0.31%. The average density is 2.97 g/cm³.

The samples were all taken from a cylindrical core drilled from a piece of granite stone which has uniform texture and were cut into normative $\Phi (50 \pm 2) \times (100 \pm 2)$ mm cylinders.

Samples are as shown in Figure 1a. The dimensions of the sample for the Brazilian test are a standard $(50 \pm 2) \text{ mm} \times (25 \pm 2) \text{ mm}$ cylinders.

For this study, dry granite is exposed to temperatures of 250 °C, 350 °C, 450 °C, 550 °C, and 650 °C and the granite underwent many cycles of heating and then cooling with water, and then the mechanical properties of each sample were examined. Each sample underwent 0, 1, 5, 10, 15 and 20 cycles of heating and then cooling with water for each temperature respectively. Zero (0) denotes that the sample is naturally cooling at room temperature.

The samples were heated to the set temperature in a high-temperature furnace (type MXQ 1700) made in Shanghai (Micro-X Furnace Co. Ltd. (Shanghai, China)) at the rate of 10 °C/min and were maintained at the designated temperature for 2 h. The heating furnace has high precision of temperature control such that control accuracy error is ± 1 °C, which meets the requirements of these experiments, as shown in Figure 1b. Then, the samples were quickly taken out of the furnace by the crucible tongs and placed in a container filled with cold water and cooled to room temperature and dried. In this process, the contact temperature of the sample with cold water will be lower than the set temperature, which will influence the experimental results. This procedure represents one cycle of heating and then cooling with water. Figure 2 shows the scheme of circulating heating and water cooling of the sample.



Figure 1. Granite sample and high-temperature furnace. (a) Granite samples; (b) High-temperature furnace.

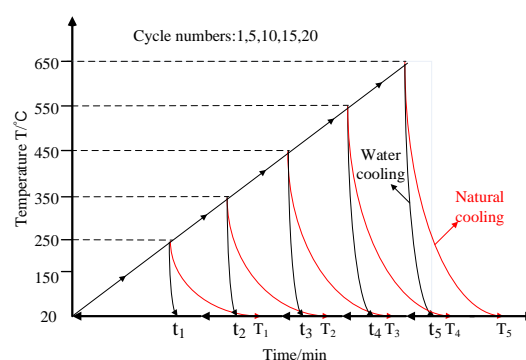


Figure 2. Test scheme of cyclic heating and cooling with circulating water.

2.2. Experimental Equipment

As shown in Figure 3, the experimental system comprises a loading system and a data acquisition system. The loading system is an MTS816 servo hydraulic testing machine that is located at the China University of Mining and Technology. The MTS816 testing machine has stable performance and a sensitive control system, and it is the most advanced laboratory testing equipment for rock mechanics in the world. The loading method is displacement control and the loading speed is 0.002 mm/min.

Prior to carrying out the uniaxial compression test, the sample was coated with a layer of lubricant to reduce the friction between the sample and the pressure head. The loading and data acquisition system mainly recorded the stress strain, AE signals and digital images. The latter were obtained with a high-speed camera which was used to capture the evolution of fractures on the samples during loading, while a DS2 acoustic emission signal analyzer recorded the AE signals of the samples.

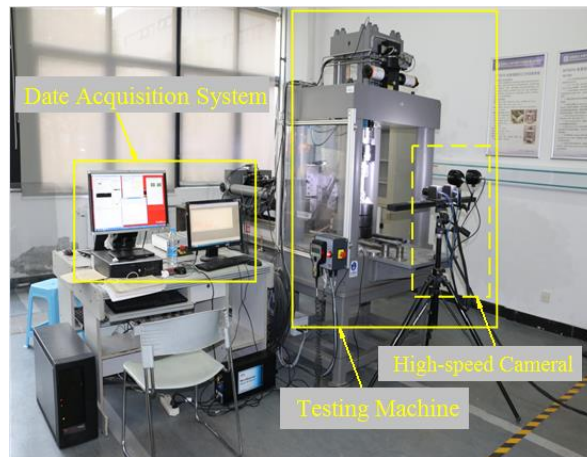


Figure 3. Experimental loading and data acquisition system.

3. Results and Discussion

3.1. Characteristics of Mechanical Strength of Granite

The stress-time curves of the two samples exposed to a temperature of 250 °C under uniaxial compression are shown in Figure 4a. The plot shows that the average peak strength, failure time, and average and secant modulus of the two samples are 123.09 MPa, 552.5 s, and 99.69 GPa and 69.25 GPa respectively, and the dispersion coefficients are 1.99×10^{-2} , 0.90×10^{-2} , 2.92×10^{-3} and 1.34×10^{-2} respectively. Figure 4b shows that the average tensile strength and failure time are 4.765 MPa and 119 s, respectively, and their dispersion coefficients are 0.11×10^{-2} and 3.4×10^{-2} respectively. The granite used in this study is quite homogeneous and the mechanical parameters show few differences, so the granite is suitable for quantitative analysis of its mechanical properties after cyclic heating and cooling. It can be seen from Figure 4 that there is no obvious yielding, which shows that the granite samples are highly brittle.

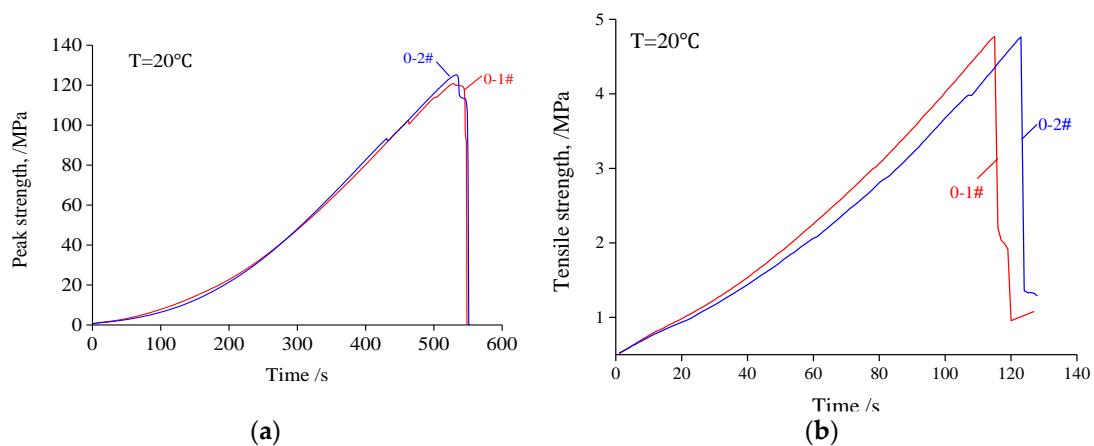


Figure 4. Peak and tensile intensity changes with time. (a) Peak intensity changes with time; (b) Tensile strength changes with time.

Figure 5a–e are plots of the strength of granite versus a different number of cycles of heating and cooling with circulating water at temperatures of 350 °C, 450 °C, 550 °C and 650 °C respectively. Figure 5f shows the peak strength based on the acoustic intensity test (peak intensity) at different temperatures and Figure 5g is the ratio of the peak strength after cooling with water to peak strength after cooling in air. Figure 5a–e show that the uniaxial compression of granite undergoes three stages of changes: pore compression, and elastic and strain softening deformations. Figure 5f shows that the cycles with water cooling have a significant effect on the peak strength of the granite and therefore cracking. With an increase in the number of cycles and increases in temperature, the elasticity and characteristics of the samples are gradually reduced and their strain softening behavior is increased. Therefore, with temperature increases, the granite is transformed from brittle to plastic. Figure 5a shows that at a temperature of 250 °C, the peak strength of the sample is 111.66 MPa while the peak intensity is 103.16 MPa after one cycle of heating and cooling with circulating water; the difference between the peak strength and peak intensity of the sample is 7.61%. The samples are very brittle. After 5 cycles of heating and cooling with circulating water, the peak strength before cracking of the sample of 90.51 MPa is equal to 81.06% of the peak strength of the sample after air cooling; the sample is obviously less brittle. After 5 cycles, the sample begins to transform from brittle to plastic. After 10 cycles, the peak strength of the sample is 71.69 MPa, which is equal to 64.20% of the peak strength of the sample after air cooling, and the material becomes obviously more plastic. After 15 and 20 cycles, the peak strength of the samples is 52.91 MPa and 50.52 MPa respectively, which is equal to 47.38% and 45.25% of the peak strength of the samples after air cooling. The samples obviously become more plastic, and the declining of the peak strength has stopped. The range of peak strengths that results in cracking is reduced after 15 cycles of heating at 250 °C and cooling with circulating water, and tends toward a constant.

The transformation from brittleness to ductility is not only affected by the number of cycles of heating and cooling with circulating water, but also the temperature. Figure 4a–e show that when the samples undergo 15 cycles at a temperature that is under 250 °C, there are no signs of brittle failure, but the material becomes more plastic. At temperatures of 350 °C, 450 °C, 550 °C, and 650 °C, the samples become more plastic after 5, 1, 1 and 0 cycles of heating and cooling with circulating water, respectively. Therefore, during the cycles, temperature plays a decisive role in the brittle to plastic transformation of granite. Figure 5f shows that with an increase in the number of cycles, the peak strength of granite at 250 °C decreases linearly. When the number of cycles is increased from 10 to 20, the peak strength shows a downward trend. With 20 cycles, the peak strength of the granite at temperatures of 350 °C to 650 °C undergoes three stages: Stage I is the rapid decline of the peak strength, Stage II is when the decline of the peak strength is reduced, and in Stage III, the peak strength is constant. In all three stages, there are further gradual decreases in the peak intensity of the samples with increases in temperature. The plot in Figure 5f is fitted with an exponential function in accordance with the parameters in Table 1.

Table 1. Fitting formulas of mechanical parameters after cyclic heating and cooling with circulating water.

Temperature	Mechanical Parameters	Fitting Formula (N:Cycle Numbers)	R ²
250 °C	Peak stress	$\sigma_{\max} = 122.16 \exp(-N/25.55) - 11.69$	0.9921
350 °C	Peak stress	$\sigma_{\max} = 60.65 \exp(-N/5.24) + 42.04$	0.9337
450 °C	Peak stress	$\sigma_{\max} = 38.93 \exp(-N/11.34) + 34.45$	0.9056
550 °C	Peak stress	$\sigma_{\max} = 19.31 \exp(-N/6.56) + 37.24$	0.8518
650 °C	Peak stress	$\sigma_{\max} = 9.25 \exp(-N/0.31) - 6.79 \exp(N/6.17) + 6.79$	0.8674

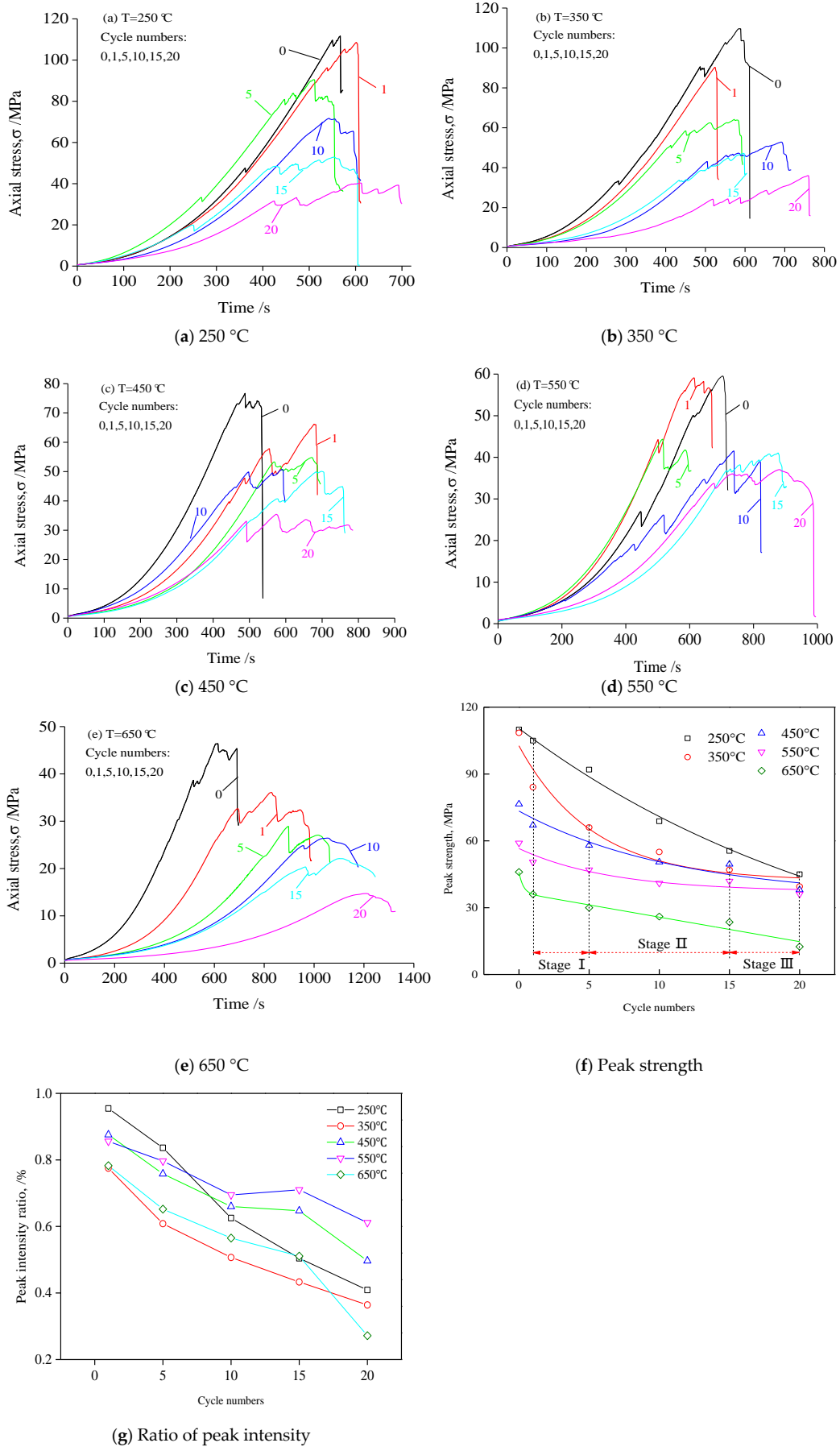


Figure 5. Strength curve and peak strength of granite.

3.2. Mechanical Tensile Strength of Granite after Cyclic Heating and Cooling with Circulating Water

Figure 6a shows that the tensile strength of granite is significantly reduced with increased number of cycles, and the effect of temperature on the tensile strength of granite is significant. After 10 cycles, cracking due to reduced tensile strength of the sample is minimal at a heating temperature of 250 °C, in which the tensile strength of the samples is reduced from 4.57 MPa to 4.39 MPa. The rate of cracking with lower tensile strength is higher at higher temperatures. This is especially true of the sample that was exposed to a temperature of 650 °C, in which the tensile strength is reduced from 2.22 MPa to 0.80 MPa, or a reduction of 64.19%. After 10 to 20 cycles, the rate of cracking with lower tensile strength is high at 250 °C; however, the tensile strength of the sample is slowly reduced with higher heating temperatures, in particular 650 °C, so that the rate of cracking is slowly increased. Thus, the cycles of heating and cooling with circulating water of granite carried out at high temperatures have a very significant impact on its tensile strength.

The tensile strength data from several experiments [37–39] are compared with the results of this study is shown in Figure 6b. It is observed that a faster rate of decline occurs at temperatures higher than 450 °C from Figure 6b. This is caused by changes in the internal structure of the granite minerals as a result of the heat. The volume expansion of quartz has increased dramatically between 450 and 550 °C. Due to the rapid expansion in the quartz volume, cracks occur between the quartz, feldspar and hornblende, causing the rapid decline in the strength at this stage.

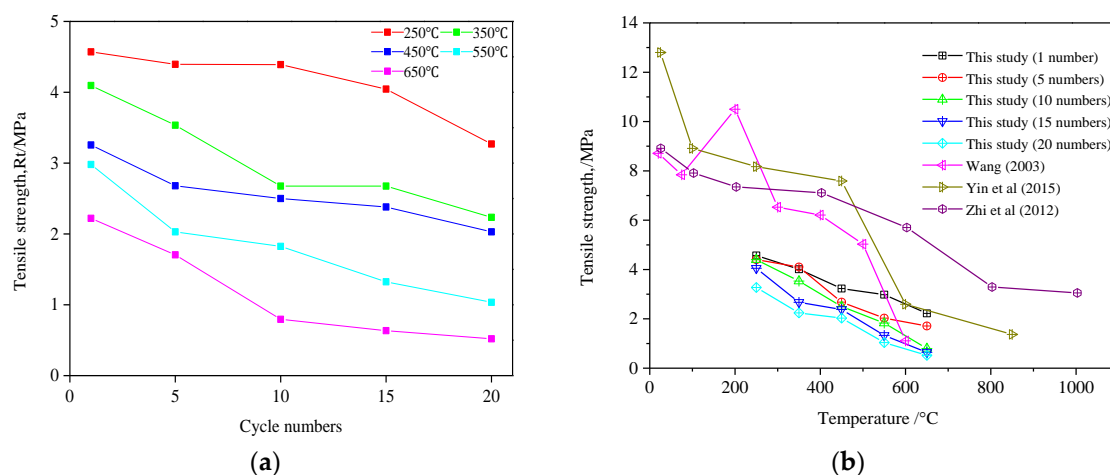


Figure 6. Tensile strength of granite after different temperature and cyclic treatment. (a) Tensile strength of granite; (b) Comparison of tensile strength of granite.

3.3. AE Characteristics of Rock Samples after Cyclic Heating and Water Cooling

AE impact is a signal whose amplitude exceeds the threshold value. The data obtained by the monitoring channel, the number of signals detected at a certain time, is the number of AE collisions, and the cumulative number of AE impacts is the cumulative number of impacts at each stage. The number of impacts which has a good correspondence with the development, expansion, confluence and transfixion of cracks in rocks reflects the activity of AE from rocks [19]. In this paper, we only analyze AE parameters of granite specimens under uniaxial compression after cyclic heating and cooling at 250 °C because of the length of the article. Figure 7 is the stress-time curve and AE characteristic curve of rock sample after cyclic heating and cooling at 250 °C.

Figure 7a is the rock sample in the natural state of cooling, i.e., the number of cycles is 0. In the initial compaction stage (oa), the number of AE collisions is small, which is generated by the closure of a small number of primary cracks, and the AE collisions are in a quiet period. Starting from the elastic stage (segment ab), the number of impacts began to increase, and a smaller number of AE events occur, and the number of AE stabilizes at a lower level. When entering the stable crack propagation

stage (bc), the number of impacts increases rapidly, and a large AE event occurs, which indicates that the cracks in the rock sample are gradually expanding and converging, and the AE number enters the active period. When entering the unstable crack propagation stage (cd), the number of impacts suddenly rises to the peak, and the cumulative number of AE rises steeply. At point d of peak intensity, the maximum number of AE impacts is reached, and the rock sample corresponds to the penetration of macroscopic cracks after the peak (de), and the number of impacts decreased, but there was still a small amount of AE activity and maintained a high level. Figure 7a shows two stress drops in the stress curve. New macroscopic cracks can be observed during each stress drop during the test and meanwhile many AE events will appear on the AE characteristic curve showing that AE monitoring can reflect the rock damage process accurately.

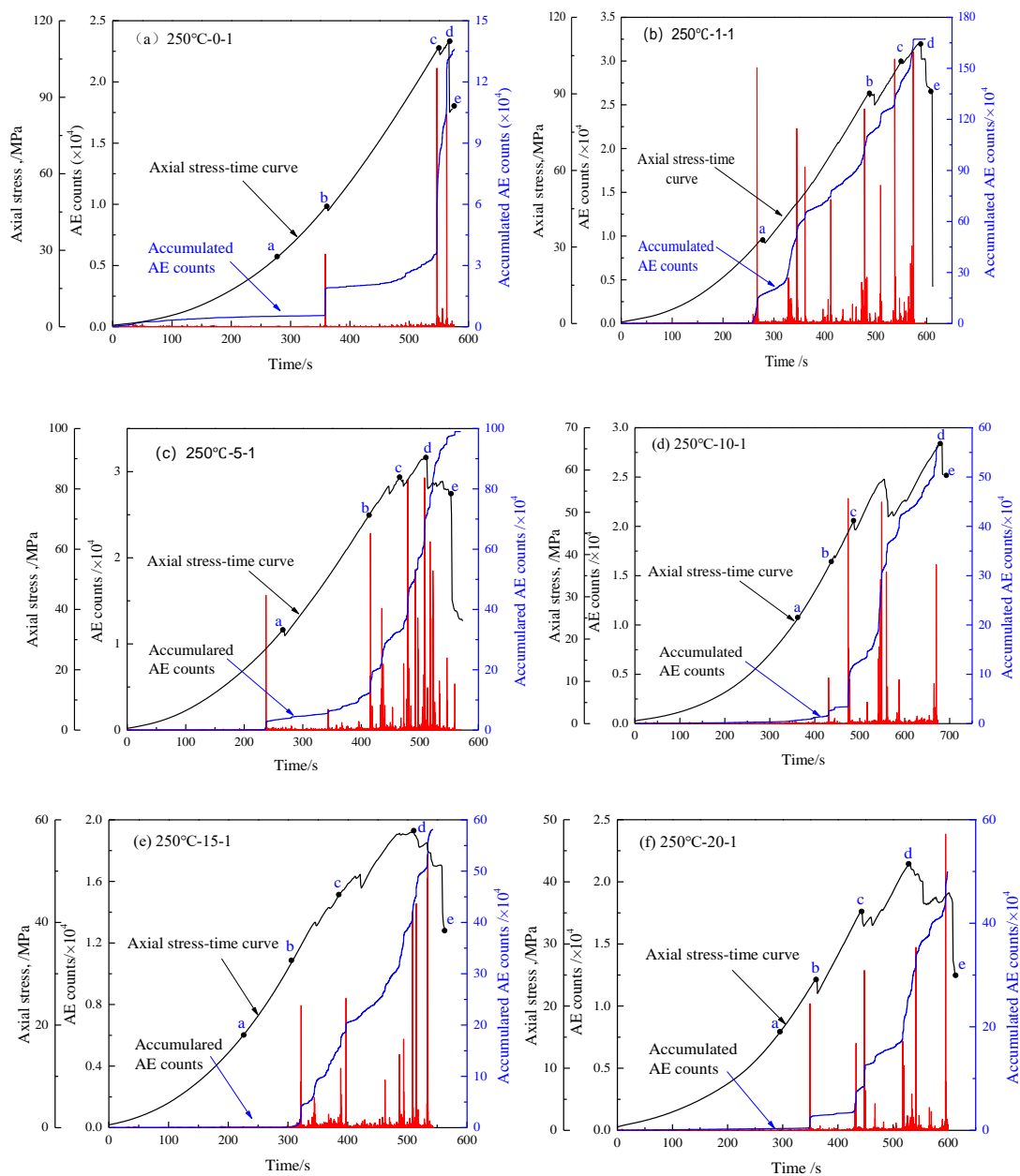


Figure 7. AE counts and accumulated of granite specimens with respect to cycle numbers at 250 °C.

As shown in Figure 7b–f, the AE characteristics of rock samples after circulating high temperature and water cooling, especially those after 10 cycles, are significantly different from those of cooling rock

samples under natural conditions. Rock samples have very few AE signals at the initial compaction stage, indicating that there are fewer AE collisions, which indicates that the thermal damage caused by repeated high temperature and water cooling is greater and the internal pores and fractures of the rock sample are damaged. The number of impacts remained low when entering the elastic stage and AE numbers entered the quiet period. When the rock sample enters the stable crack propagation stage, the number of impacts increases, and the acoustic emission event is in the active period, which can be distinguished from the elastic phase; however, the AE activity of rock samples is not as strong as that of natural cooling. When the rock sample enters the unstable crack propagation stage, the number of AE collisions will suddenly rise to a small peak, but the increase degree of impact number is not as severe as that of natural cooling. The number of impacts does not reach the peak when the stress reaches the peak intensity, but lags behind the peak intensity. In general, after several cycles of high temperature and water cooling, the initial damage of rock sample becomes bigger and makes the AE signal inactive at the initial stage of loading. Because the thermal fracture increases the ductility of rock samples, starting with the elastic phase, AE impingement is less active than natural cooling, so the gradual failure process becomes slower than that of natural cooling as strain increases. With the increase of the number of cycles of high temperature and water cooling, the number of AE events accumulated in the sample under uniaxial compression decreased.

3.4. Rock Damage Analysis

3.4.1. Uniaxial Compression Mechanical Damage

Since the evolution of rock micro-defects is a random change, it can be considered that the strength distribution of microelements obeys Weibull distribution, and its distribution density function is:

$$\varnothing\varepsilon = m/\alpha\varepsilon^{m-1} \exp(-\varepsilon^m/\alpha), \quad (1)$$

$\varnothing\varepsilon$ is micro-element damage rate of sample under loading. Because the law of AE activity is basically consistent with the statistical distribution of internal defects of materials, when the whole cross section of the damage accumulation of AE is Ω_m , the accumulated AE of the sample compressed to destroy is:

$$\Omega = \Omega_m \int_0^\varepsilon \varnothing(x)dx, \quad (2)$$

Equation (1) is substituted into Equation (2) and then integrated to get Equation (3):

$$\Omega/\Omega_m = 1 - \exp(-\varepsilon^m/\alpha), \quad (3)$$

There is the following relationship between the damage parameter D and the probability density of micro-element failure:

$$D = \int_0^\varepsilon \varnothing(x)dx = 1 - \exp(-\varepsilon^m/\alpha), \quad (4)$$

Compared with Equation (3) and Equation (4), the uniaxial compression mechanical damage can be obtained as follows:

$$D = \Omega/\Omega_m, \quad (5)$$

Mechanical damage curves of rock samples at different temperatures are drawn based on AE experimental data, as shown in Figure 8, which shows that in the initial compaction stage, the primary pores and fractures in granite are compacted, and the damage variable is almost 0. Then, the damage variable increases slightly, and the deformation damage in this stage is mainly caused by elastic deformation of rock sample mineral particles. The mechanical damage of rock samples in these two stages is less affected by temperature and water-cooling times N . The rock is in the stage of unstable fracture when the stress reaches about 60% of the ultimate strength. The damage variable increases rapidly because of friction, dislocation occurs between granite particles, and new cracks

occur. Therefore, $0.6\sigma_b$ can be used as the threshold stress value of granite damage [40]. When the ultimate strength is exceeded, the damage value gradually approaches 1 and the rock sample tends to be damaged. At the same time, it can be seen from Figure 8 that under the same temperature and stress, the mechanical damage becomes greater with the increase of the number N of high temperature and water cooling, indicating that high temperature and water cooling have caused thermal damage to the rock sample.

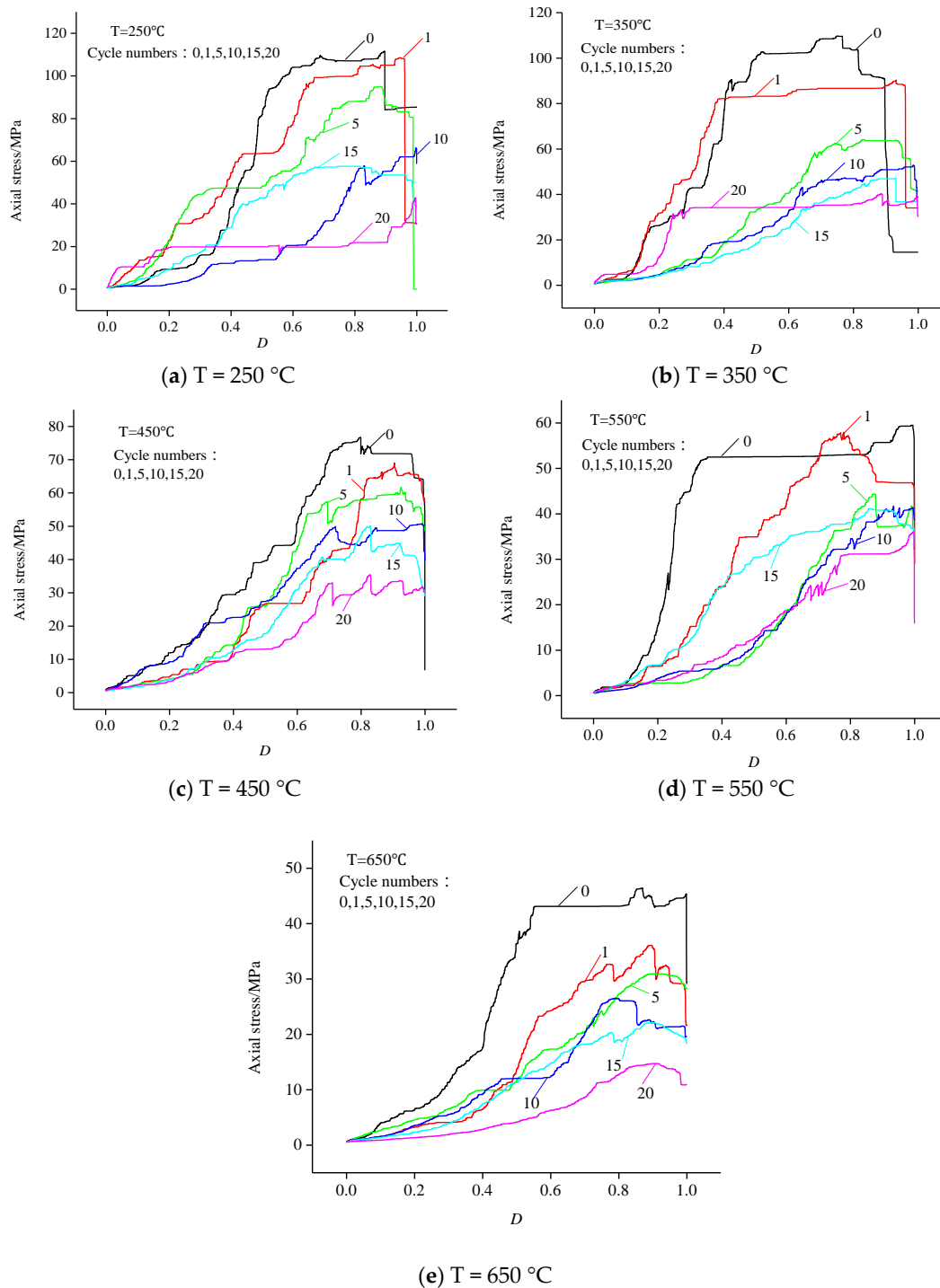


Figure 8. Mechanical damage curve of samples after circulating high temperature and cooling water.

3.4.2. Heat Shock Damage of High Temperature and Cold Water

The elastic modulus is taken as the damage variable of rock sample to characterize the effect of the numbers of cyclic heating and water cooling on the mechanical properties of rock. Thermal shock damage of rock sample is 0 when the specimen is in the natural state at 25 °C. The elastic modulus of each sample at each test temperature was treated after 20 cycles of heating and water cooling; the thermal shock damage factor was defined as follows:

$$DT = 1 - E_T^{(N)} / E_0, \quad (6)$$

In the above formula, $E_T^{(N)}$ is the elastic modulus of granite after N times of circulating water cooling at temperature T , E_0 is the elastic modulus of granite in its natural state at 25 °C, shock damage D of heat–water at different temperatures is shown in Figure 8 and the damage fitting equation is shown in Table 2.

Table 2. Fitting curve equations of damage D value and cycle number N of samples.

Temperature	Thermal Shock	Fitting Formula (N :Cycle Numbers)	R^2
250 °C	D	$D = -0.0168 N + 0.0124 N^2 - 9.69 \times 10^{-2} N^3 + 2.261 \times 10^{-5} N^4$	0.9902
350 °C	D	$D = -0.0916 N - 0.004 N^2 + 8.47 \times 10^{-6} N^3 + 3013 \times 10^{-6} N^4$	0.9997
450 °C	D	$D = 0.0693 N - 0.0065 N^2 + 3.25 \times 10^{-4} N^3 - 5.868 \times 10^{-6} N^4$	0.9654
550 °C	D	$D = 0.0274 N + 0.0015 N^2 - 2.50 \times 10^{-4} N^3 + 6.94 \times 10^{-6} N^4$	0.9943
650 °C	D	$D = 0.08975 N - 0.01308 N^2 + 7.88 \times 10^{-4} N^3 - 1.614 \times 10^{-5} N^4$	0.9675

As can be seen from Figure 9, the D value of specimen damage increases with the increase of N at the same temperature. This is due to the appearance of tiny cracks in the surface of the granite specimen during the cold and thermal cycle, which is spread throughout the whole sample, cutting the rock mass and destroying the internal structure of the specimen leads to the reduction of the bearing capacity of the rock. The surface rock of the specimen is further softened by water action, which increases the accumulation of irreparable deformation, leads to the further expansion of the existing crack depth and the increases of the number of cracks, so the damage value increases gradually when the structural connection of rock is destroyed. At the same number of cycles of high temperature and cold water and as the temperature goes up, the damage value N gradually increases because the thermal tensile stress of granite exceeds the tensile strength of the material itself, the material will undergo thermal damage. The higher the temperature of the specimen itself, the greater the tensile stress on its surface. Tensile cracks will occur on the surface of the specimen when the tensile strength of the rock exceeds the tensile strength. The external temperature of the specimen decreases sharply but the internal temperature is relatively high during rapid cooling, the tensile crack on the surface of specimen and the excess part of material is caused by external shrinkage and internal expansion. In the heating process, more dorsal cracks are produced at the excess part of the material due to external expansion and internal contraction. Because the external temperature rises sharply, and the internal temperature decreases relatively, there will be more tiny cracks in the rock than expected.

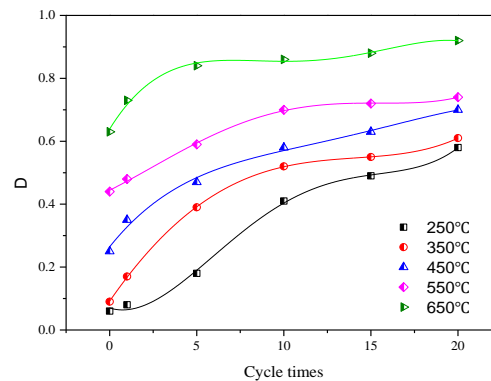


Figure 9. Samples damage fitting curve.

3.4.3. The Cracking Mechanism of Granite under High-Temperature and Cold-Water Impact

The total strain of the rock samples under different temperatures after cooling by cold water is ε . Suppose the rock sample contains n kinds of mineral particles, the thermal expansion coefficient of each mineral particle after N cycles of cold and heat is $\alpha_1^{(N)}, \alpha_2^{(N)} \dots \alpha_i^{(N)} \dots \alpha_n^{(N)}$, the elastic modulus are $E_1^{(N)}, E_2^{(N)} \dots E_i^{(N)} \dots E_n^{(N)}$ respectively. Suppose the granite sample is elastic material, the stress of each mineral particle in the sample after repeated heating and cooling can be obtained as follows:

$$\sigma_1^{(N)} = E_1^{(N)}(\alpha_1^{(N)}\Delta T - \varepsilon), \sigma_2^{(N)} = E_2^{(N)}(\alpha_2^{(N)}\Delta T - \varepsilon) \dots \sigma_i^{(N)} = E_i^{(N)}(\alpha_i^{(N)}\Delta T - \varepsilon) \dots \sigma_n^{(N)} = E_n^{(N)}(\alpha_n^{(N)}\Delta T - \varepsilon), \quad (7)$$

Due to in the process of rapid cooling there is only thermal shock and there is no other external force, the following Equation (8) can be established according to the mechanical equilibrium condition:

$$\sum_{i=1}^n E_i^{(N)} (\alpha_i^{(N)} \Delta T - \varepsilon) = 0 \quad (8)$$

The total strain ε can be solved by Equation (8):

$$\varepsilon = \frac{\sum_{i=1}^n E_i^{(N)} \alpha_i^{(N)} \Delta T}{\sum_{i=1}^n E_i^{(N)}}, \quad (9)$$

Substituting the strain ε into the stress expressions, the thermal shock stress of each mineral particle is:

$$\sigma_i^{(N)} = E_i^{(N)} \Delta T \left[\frac{\sum_{j=1}^n E_j^{(N)} (\alpha_i^{(N)} - \alpha_j^{(N)})}{\sum_{i=1}^n E_i^{(N)}} \right] \quad (10)$$

In the process of high-temperature water cooling of rock sample, the compressive stress of highly deformed mineral particles is σ_{ic} , and the tensile stress of small deformed mineral particles is σ_{it} . Suppose σ_c and σ_t are the compressive strength and tensile strength of rock sample respectively. When $\sigma_{ic} \geq \sigma_c$ or $\sigma_{it} \geq \sigma_t$, thermal cracking occurs in rocks. Because granite is a relatively dense rock, when it is heated at high temperature and cooled by water, the deformation of mineral particles cannot be developed freely to a certain extent and the thermal stress of the structure is large. As a result, micro-fractures in rock samples increase. The deformation of mineral particles cannot be developed freely to a certain extent due to granite being a relatively dense rock during high-temperature heating and water cooling, therefore, the thermal stress of the structure produced by the particles is large, leading to the increase of micro-cracks in the rock sample. Even without external force, the thermal stress of the structure in rock sample increases with temperature is obvious. From what has been discussed above, after N cycles of high temperature and water cooling, the change from the original

complete structure to the fractured rock structure caused by thermal shock stress accumulation is the main reason of rock strength damage.

3.5. Failure Mode of Granite at Different Temperatures

As shown in Figure 10a, brittle shear failure of the granite occurs after 1–10 cycles of heat treatment at 250 °C, such that the sample is broken into pieces. At the moment of failure, the sample releases large amounts of elastic energy, and breaks into large pieces, and the AE signals immediately increase. After 10 cycles, the brittleness of the samples is gradually reduced. During uniaxial loading, shear failure occurs in the granite, there is spalling on the surface, and no significant changes in the color of the sample.

As shown in Figure 10b, brittle failure occurs in the granite samples at a temperature of 350 °C after 1 to 5 cycles of heating and cooling with water. Slipping of the shear surface is mainly found in the samples, but the amount of damage is significantly reduced, and results in flaking and spalling in the middle of the sample. After 10–15 cycles, there is plastic failure of the samples, and the middle part flakes first during uniaxial loading. During the failure process, there is an increase in granite powder which shows that there is slipping of the shear surface. After 20 cycles, the color of the samples changes from a gray to pale yellow color.

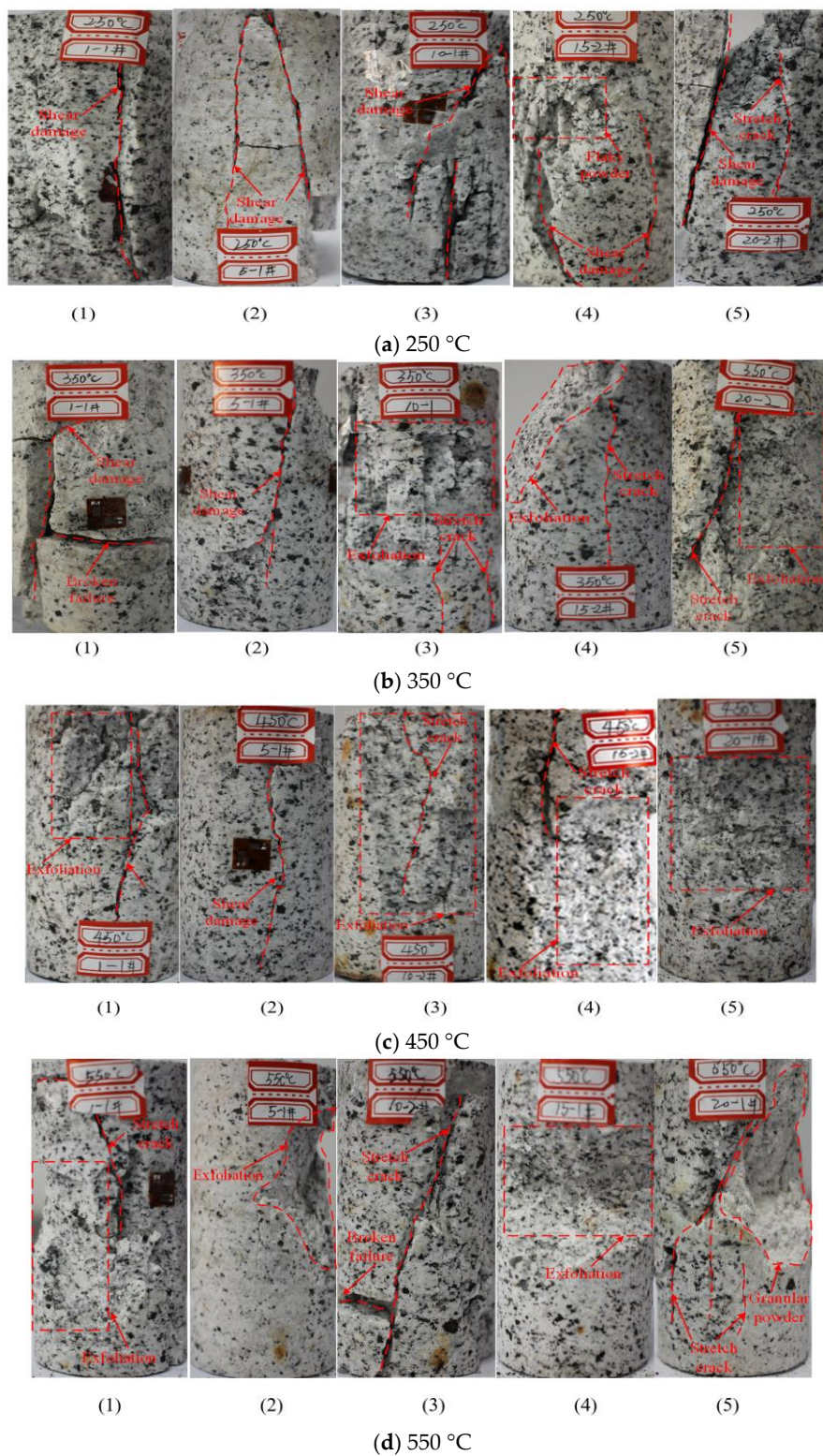


Figure 10. Failure mode of granite after cyclic heating and cooling with circulating water.

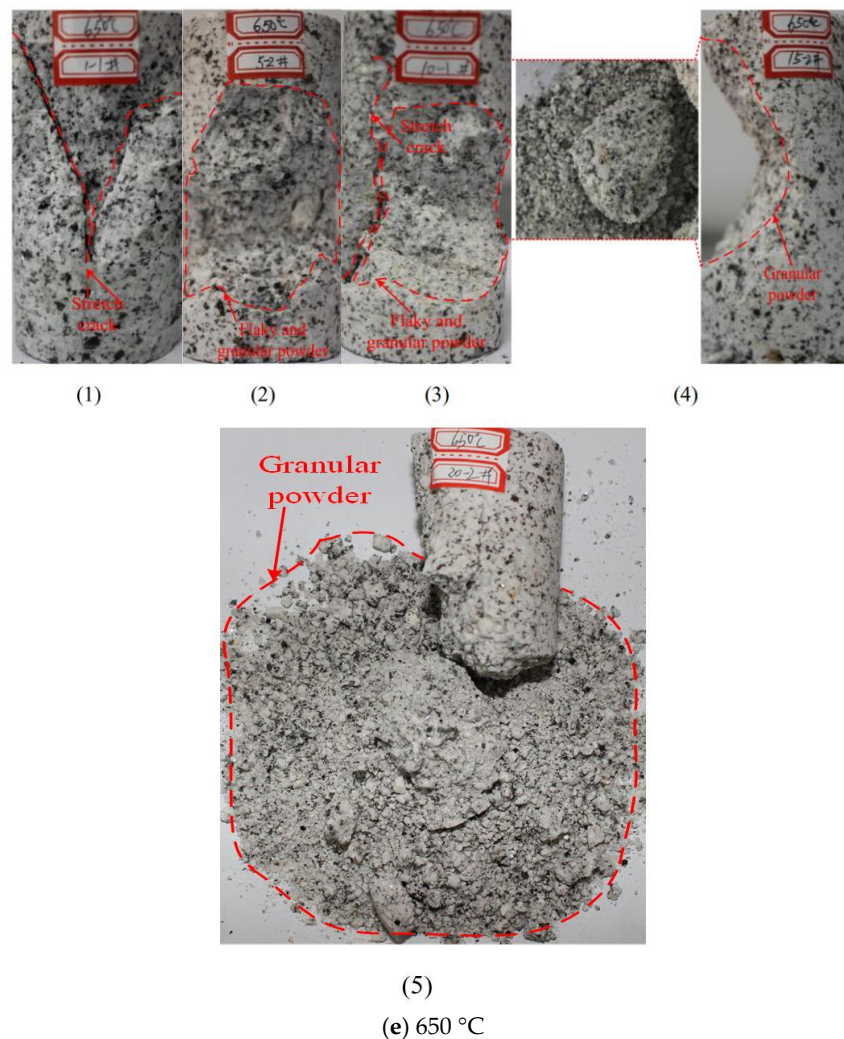


Figure 10. Cont.

In Figure 10c,d, there is brittle failure of the granite samples at temperatures of 450 °C and 550 °C after 1 cycle and cracks are found on the samples. Shear failure is found in the samples under uniaxial compression, but there is release of the elastic energy and therefore the amount of damage is significantly less, with flaking of a small area of the surface material. After 5 cycles, plastic failure occurs in the samples, and the middle of the sample flakes first under uniaxial loading, and then there is spalling in the middle of the sample. In the process of failure, the size of the granite powder particles increases significantly with less shear slipping of the sample while incurring more shear failure. The color of the samples gradually changes from gray to yellow and then to pale yellow.

The mechanical parameters of granite at a temperature of 650 °C in Figure 10e are obviously changed after air cooling from brittle to plastic. After 1 cycle, a cross shear failure surface develops with a smaller number of layered blocks of granite. After 5 cycles, uniaxial loading causes the sample to change from flaking/spalling to particle detachment, and shows layers of a failed surface. With increases in the number of cycles, failure appears in the center of the sample. After the sample has undergone 15 cycles, the material has lost most of the cohesion and bonding between particles and the granite is changed to a granular material. After 5 cycles, the color of the sample changes from gray to light yellow and then to dark yellow.

In summary, the heat treatment temperature and cycles of heating and cooling with circulating water have important impacts on the failure mode of granite, with greater impacts on the internal structure of the granite at higher temperatures when rapid cooling with water takes place. The force of

the thermal shock produces new cracks in the granite, and elongates the previous cracks. In addition, the granite particles are less compact when cooled rapidly with water, which is also the reason for the transformation of the granite from brittle to plastic. Thermal shock occurs during cycles of heating and cooling with circulating water at high temperatures. Higher temperatures result in more intense thermal shocks, as well as more obvious deterioration of the internal structure and changes in the chemical composition of the granite.

3.6. Analysis and Discussion

Figure 11 shows the normalized compressive strength data from several experiments [41–44] compared with the results of this study. Although the fluctuation of compressive strength of each type of granite is different, the normalized compressive strength can be observed decreasing below 200 °C in treatment temperature. When the treatment temperature exceeds 200 °C, the compressive strength quickly starts to decrease with increasing temperature. However, it is observed that a faster rate of decline occurs at temperatures higher than 400 °C (Figure 11). This is caused by changes in the internal structure of the granite minerals as a result of the heat. The sharp increase in the thermal expansion [45,46] of quartz at temperatures between 400 °C and 500 °C is shown in Figure 11. Due to the rapid expansion in the quartz volume, cracks occur between the quartz, feldspar and hornblende, causing the rapid decline in the strength at this stage.

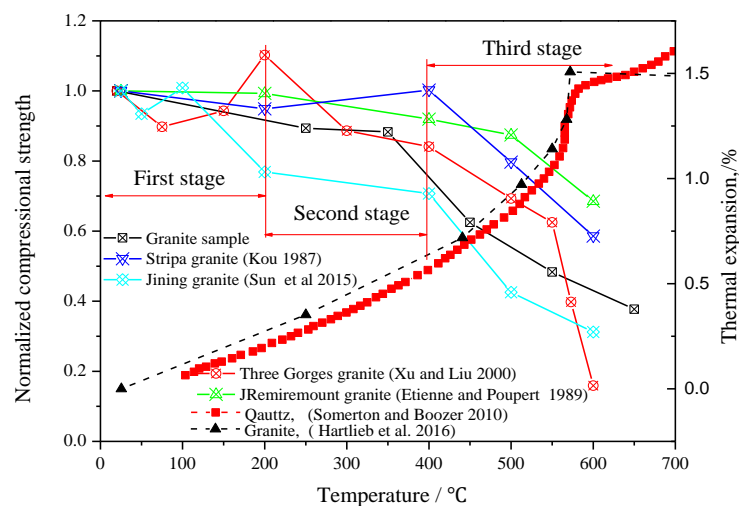


Figure 11. Differences in the normalized compressive strength of granite on different studies (source: three Gorges granite from Xu and Liu [41]; Remiremount granite from Etienne and Poupert [42]; Stripa granite from Kou [43]; Jining granite from Sun et al. [44]).

The decrease in some mechanical properties (compressive strength, and tensile strength) and the increase in the peak strain of heated granite are caused by thermally induced variations in internal structure. Because granite is composed of mineral particles with different thermal expansion coefficients and thermo-elastic characteristics, high temperature leads to inhomogeneous thermal expansion of mineral particles or the phase transition of some mineralogical components, generating internal stress and micro-cracks in granite [44]. Between 400 °C and 600 °C, and especially 500 and 600 °C, the minerals of granite have chemical changes [47]. At roughly 573 °C and under atmospheric conditions, quartz has a phase transformation from α phase to β phase, which can be used to explain the large variation of mechanical and physical properties.

The mechanical damage of samples after natural cooling from the literature [40] is compared with the results of this study as shown in Figure 12a. The mechanical damage curves of the samples studied in the literature have been obviously effected by temperature. In this paper, when the damage value of almost all samples was 0.7, the corresponding axial stress value reached the maximum. Figure 12b

shows that the fluctuation of mechanical damage value of each sample is not obvious. When the stress value is 0–30% of the peak strength, the mechanical damage value of the unheated sample is the largest, and the D value is about 0.4; when the mechanical damage value of the 550 °C sample is the smallest, and the D value is about 0.2. When the stress value reached 30% of the peak strength, the mechanical damage value of the sample began to be significantly dispersed, and the mechanical damage value was significantly affected by temperature. Compared with the mechanical damage curves of the samples in the literature, we can find that the samples in this paper will suffer greater mechanical damage at a lower stress level which shows that the samples in the literature have higher strength and brittleness than the samples in this study. We found that the influence factors of mineral composition, processing precision, heating and cooling condition and stability of loading equipment are related to the difference tests of the mechanical damage curve.

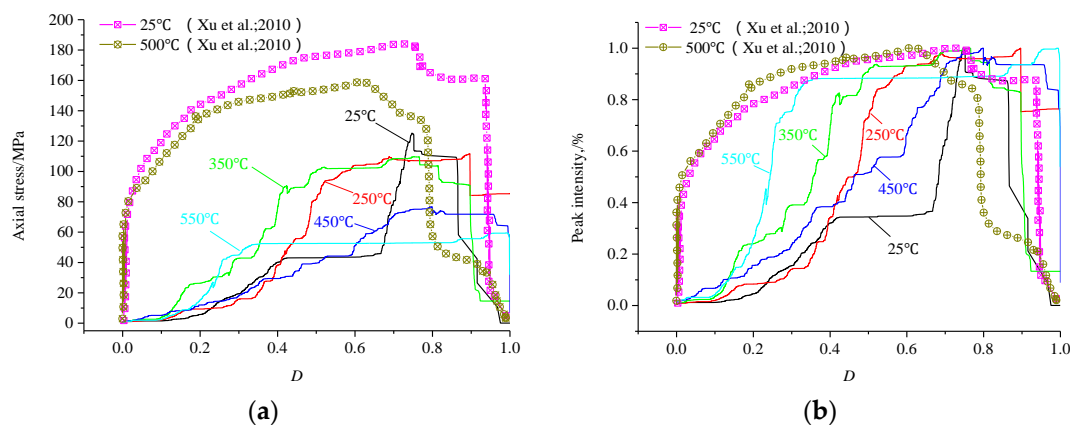


Figure 12. Mechanical damage curve of samples after natural cooling (source: Xu et al. [40]). (a) Mechanical damage curve under uniaxial compression; (b) Mechanical damage curve is represented by the ratio of axial stress to peak strength.

4. Conclusions

The following conclusions are made based on an experimental study of the mechanical properties of granite that have been exposed to temperatures from 250 °C to 650 °C under cyclic heating and cooling with circulating water, and cracking of the granite due to thermal shock with rapid water cooling.

(1) The uniaxial compression of granite undergoes three stages of changes after cyclic heating and cooling with circulating water at different heat treatment temperatures: pore compression, and elastic and strain softening deformations. The number of cycles has a significant influence on the peak stress, peak strain and uniaxial compressive strength. The transformation from brittleness to ductility is not only affected by the number of cycles, but also by the effects of temperature, which are more obvious. At a temperature of 250 °C, the granite becomes more plastic and is no longer brittle after 15 cycles. At heat treatment temperatures of 350 °C, 450 °C, 550 °C, and 650 °C, the samples become more plastic after 5, 1, 1 and 0 cycles, respectively. After heating and cooling with circulating water, the samples become even more plastic. During the cycles, temperature is seen to play a decisive role in the transformation of the granite samples from brittle to plastic.

(2) After cyclic heating and cooling with circulating water, the peak strength of the granite at different temperatures decreases, which can be described in three stages: Stage I is the rapid decline of the peak strength, Stage II is when the decline of the peak strength is reduced, and in Stage III, the strength of the sample is basically maintained at a constant level.

(3) The AE curve agrees well with the stress-time curve at each test temperature point, thus, mechanical damage can be defined by rock sample AE ringing counting rate and the threshold stress of rock damage is about 60% of the strength limit. The mechanical damage increases with the

increase of N water cooling at high-temperature cycles under the same stress. The thermal damage defined by the elastic modulus is generally increased, and can be synthesized by the four-order curve equation. The thermal stress of granite after cyclic high temperature and water cooling is caused by the thermal expansion effect of mineral particles in the structural composition and the thermal stress equation of particle structure was established, the main causes of damage were analyzed based on damage-cracking theory.

(4) With increases in the treatment temperature and more cycles of heating and water cooling, the failure mode of the granite transforms from brittle to plastic. The failure mode is transformed from slipping of the shear surface to flaking and particle spalling, and the color of the samples changes from gray to pale yellow. The temperature therefore affects the failure mode of the granite.

This paper attempts to study the mechanical parameter damage of granite samples after cyclic heating and cooling with cool water. However, the complexity of rock structures may lead to scattered data during experiments, so the interferences introduced by individual differences among the samples cannot be excluded. Therefore, these conclusions need further experiments for validation, and further investigation on their applicability under various conditions, so that more test methods can be developed for recognizing the damage process of rock failure.

Author Contributions: D.Z., H.J., Q.Y. and G.H. conceived and designed the experiments; D.Z. and Q.Y. performed the experiments; D.Z. and G.H. analyzed the data; H.J. contributed laboratory equipment; D.Z. and Q.Y. wrote the paper.

Funding: This research was funded by the National Natural Science Foundation of China (Grant Nos. 51734009, 51709260, 51704279), and the Natural Science Foundation of Jiangsu Province, China (No. BK20170276).

Conflicts of Interest: The authors declare no conflict of interest.

References

- Nicholson, K. Environmental protection and the development of geothermal energy resources. *Environ. Geochem. Health*. **1994**, *16*, 86–87. [[CrossRef](#)] [[PubMed](#)]
- Liu, R.; Li, B.; Jiang, Y. Critical hydraulic gradient for nonlinear flow through rock fracture networks: The roles of aperture, surface roughness, and number of intersections. *Adv. Water Resour.* **2016**, *88*, 53–65. [[CrossRef](#)]
- Liu, R.; Li, B.; Jiang, Y. A fractal model based on a new governing equation of fluid flow in fractures for characterizing hydraulic properties of rock fracture networks. *Comput. Geotech.* **2016**, *75*, 57–68. [[CrossRef](#)]
- Liu, R.; Jiang, Y.; Li, B.; Wang, X. A fractal model for characterizing fluid flow in fractured rock masses based on randomly distributed rock fracture networks. *Comput. Geotech.* **2015**, *65*, 45–55. [[CrossRef](#)]
- Li, B.; Liu, R.; Jiang, Y. Influences of hydraulic gradient, surface roughness, intersecting angle, and scale effect on nonlinear flow behavior at single fracture intersections. *J. Hydrol.* **2016**, *538*, 440–453. [[CrossRef](#)]
- Tapponnier, P.; Brace, W.F. Development of stress-induced microcracks in Westerly Granite. *Int. J. Rock Mech. Min. Sci. Geomech. Abstr.* **1976**, *13*, 103–112. [[CrossRef](#)]
- Wair, R.S.C.; Lo, K.Y.; Rowe, R.K. Thermal stress analysis in rock with nonlinear properties. *Int. J. Rock Mech. Min. Sci. Geomech. Abstr.* **1982**, *19*, 211–220.
- Simpson, C. Deformation of granitic rocks across the brittle-ductile transition. *J. Struct. Geol.* **1985**, *7*, 503–511. [[CrossRef](#)]
- Singh, B.; Ranjith, P.G.; Chandrasekharam, D.; Viete, D.; Singh, H.K.; Lashin, A.; Arifi, N.A. Thermo-mechanical properties of Bundelkhand granite near Jhansi, India. *J. Geomech. Geophys. Geo-Energy Geo-Resour.* **2015**, *1*, 35–53. [[CrossRef](#)]
- Sygała, A.; Bukowska, M.; Janoszek, T. High Temperature Versus Geomechanical Parameters of Selected Rocks—The Present State of Research. *J. Sustain. Min.* **2013**, *12*, 45–51. [[CrossRef](#)]
- Ranjith, P.G.; Viete, D.R.; Chen, B.J.; Perera, M.S. Transformation plasticity and the effect of temperature on the mechanical behaviour of Hawkesbury sandstone at atmospheric pressure. *Eng. Geol.* **2012**, *151*, 120–127.
- Araújo, R.G.S.; Sousa, J.L.A.O.; Bloch, M. Experimental investigation on the influence of temperature on the mechanical properties of reservoir rocks. *Int. J. Rock Mech. Min. Sci.* **1997**, *34*, 298.e1–298.e16. [[CrossRef](#)]
- Su, H.; Jing, H.; Du, M.; Wang, C. Experimental investigation on tensile strength and its loading rate effect of sandstone after high temperature treatment. *Arab. J. Geosci.* **2016**, *9*, 616–627. [[CrossRef](#)]

14. Meng, X.; Liu, W.; Meng, T. Experimental Investigation of Thermal Cracking and Permeability Evolution of Granite with Varying Initial Damage under High Temperature and Triaxial Compression. *Adv. Mater. Sci. Eng.* **2018**, *4*, 1–9. [[CrossRef](#)]
15. Chen, S.; Yang, C.; Wang, G. Evolution of thermal damage and permeability of Beishan granite. *Appl. Therm. Eng.* **2017**, *110*, 1533–1542. [[CrossRef](#)]
16. Guo, L.L.; Zhang, Y.B.; Zhang, Y.J.; Yu, Z.W.; Zhang, J.N. Experimental investigation of granite properties under different temperatures and pressures and numerical analysis of damage effect in enhanced geothermal system. *Renew. Energy* **2018**, *126*, 107–125. [[CrossRef](#)]
17. Rong, G.; Peng, J.; Yao, M.; Jiang, Q.H.; Wong, L.N.Y. Effects of specimen size and thermal-damage on physical and mechanical behavior of a fine-grained marble. *Eng. Geol.* **2018**, *232*, 46–55. [[CrossRef](#)]
18. Yu, Q.L.; Ranjith, P.G.; Liu, H.Y.; Yang, T.H.; Tang, S.B.; Tang, C.A.; Yang, S.Q. A Mesostructure-based Damage Model for Thermal Cracking Analysis and Application in Granite at Elevated Temperatures. *Rock Mech. Rock Eng.* **2015**, *48*, 2263–2282. [[CrossRef](#)]
19. Yang, S.Q.; Ranjith, P.G.; Jing, H.W.; Tain, W.L.; Ju, Y. An experimental investigation on thermal damage and failure mechanical behavior of granite after exposure to different high temperature treatments. *Geothermics* **2017**, *65*, 180–197. [[CrossRef](#)]
20. Uetsuji, Y.; Zako, M. On Evaluation Procedure to AE Test for Fiber Reinforced Composite Materials based on Damage Mechanics. *Trans. Jpn. Soc. Mech. Eng.* **1998**, *64*, 2938–2944. [[CrossRef](#)]
21. Venturini Autieri, M.R.; Dulieu-Barton, J.M. Initial Studies for AE Characterisation of Damage in Composite Materials. *Adv. Mater. Res.* **2010**, *13–14*, 273–280.
22. Ding, Q.L.; Ju, F.; Mao, X.B.; Ma, D.; Yu, B.Y.; Song, S.B. Experimental investigation of the mechanical behavior in unloading conditions of Sandstone after high-temperature treatment. *Rock Mech. Rock Eng.* **2016**, *49*, 2641–2653. [[CrossRef](#)]
23. Watanabe, H.; Murakami, Y.; Ohtsu, M. Quantitative Evaluation of Damage in Concrete Based on AE. *J. Soc. Mater. Sci. Jpn.* **2001**, *50*, 1370–1374. [[CrossRef](#)]
24. Suzuki, T.; Ohtsu, M. Quantitative damage evaluation of structural concrete by a compression test based on AE rate process analysis. *Constr. Build. Mater.* **2004**, *18*, 197–202. [[CrossRef](#)]
25. Sagar, R.V.; Prasad, B.K.R.; Kumar, S.S. An experimental study on cracking evolution in concrete and cement mortar by the b-value analysis of acoustic emission technique. *Cem. Concr. Res.* **2012**, *42*, 1094–1104. [[CrossRef](#)]
26. Vidya Sagar, R.; Raghu Prasad, B.K. A Review of recent development in parametric based acoustic emission techniques applied to concrete structures. *Nondestruct. Test. Eval.* **2012**, *27*, 47–68. [[CrossRef](#)]
27. Wu, G.; Zhai, S.T.; Wang, Y. Research on characteristics of mesostructure and acoustic emission of granite under high temperature. *J. Rock Soil Mech.* **2015**, *36*, 351–356.
28. Chen, G.Q.; Li, T.B.; Zhang, G.F.; Yin, H.Y.; Zhang, H. Temperature effect of rock burst for hard rock in deep-buried tunnel. *Nat. Hazard* **2014**, *72*, 915–926. [[CrossRef](#)]
29. Wang, J.S.Y.; Mangold, D.C.; Tsang, C.F. Thermal impact of waste emplacement and surface cooling associated with geologic disposal of high-level nuclear waste. *Environ. Geol. Water Sci.* **1988**, *11*, 183–239. [[CrossRef](#)]
30. Jiang, L.H.; Chen, Y.L.; Liu, M.L. Experimental study of mechanical properties of granite under high/low temperature freeze-thaw cycles. *Rock Soil Mech.* **2011**, *32*, 319–323.
31. Kim, K.; Kemeny, J.; Nickerson, M. Effect of Rapid Thermal Cooling on Mechanical Rock Properties. *Rock Mech. Rock Eng.* **2014**, *47*, 2005–2019. [[CrossRef](#)]
32. Kumari, W.G.P.; Ranjith, P.G.; Perera, M.S.A.; Chen, B.K.; Abdulagatov, I.M. Temperature-dependent mechanical behaviour of Australian Strathbogie granite with different cooling treatments. *Eng. Geol.* **2017**, *229*, 31–44. [[CrossRef](#)]
33. Isaka, B.L.A.; Gamage, R.P.; Rathnaweera, T.D.; Perera, M.S.A.; Chandrasekharam, D.; Kumari, W.G.P. An Influence of Thermally-Induced Micro-Cracking under Cooling Treatments: Mechanical Characteristics of Australian Granite. *Energies* **2018**, *11*, 1338. [[CrossRef](#)]
34. Xu, X.L.; Zhang, Z.Z. Acoustic Emission and Damage Characteristics of Granite Subjected to High Temperature. *Adv. Mater. Sci. Eng.* **2018**, *4*, 1–12. [[CrossRef](#)]
35. Shao, S.; Wasantha, P.L.P.; Ranjith, P.G.; Chen, B.K. Effect of cooling rate on the mechanical behavior of heated Strathbogie granite with different grain sizes. *Int. J. Rock Mech. Min. Sci.* **2014**, *70*, 381–387. [[CrossRef](#)]
36. Rickard, H. Fire behavior of mining vehicles in underground hard rock mines. *Int. J. Min. Sci. Technol.* **2017**, *27*, 627–634.

37. Wang, G. Experiment Research on the Effects of Temperature and Viscoelastoplastic Analysis of Beishan Granite. Ph.D. Thesis, Xi'an University of Science and Technology, Xi'an, China, 2003.
38. Zhi, L.P.; Xu, J.Y.; Liu, Z.Q.; Liu, S.; Chen, T.F. Research on ultrasonic characteristics and Brazilian splitting tensile test of granite under post-high temperature. *Rock Soil Mech.* **2012**, *33*, 61–66.
39. Yin, T.B.; Li, X.B.; Cao, W.Z.; Xia, K.W. Effects of Thermal Treatment on Tensile Strength of Laurentian Granite Using Brazilian Test. *Rock Mech. Rock Eng.* **2015**, *48*, 2213–2223. [[CrossRef](#)]
40. Xu, X.L.; Gao, F.; Ji, M. Damage Mechanical Analysis of Fracture Behavior of Granite Under Temperature. *J. Wuhan Univ. Technol.* **2010**, *32*, 143–147.
41. Xu, X. A preliminary study on basic mechanical properties for granite at high temperature. *Chin. J. Geotech. Eng.* **2000**, *22*, 332–335.
42. Homand-Etienne, F.; Houpert, R. Thermally induced microcracking in granites: characterization and analysis. *Int. J. Rock Mech. Min. Sci. Geomech. Abstr.* **1989**, *26*, 125–134. [[CrossRef](#)]
43. Kou, S.Q. Effect of thermal cracking damage on the deformation and failure of granite. *Acta Mech. Sin.* **1987**, *242*, 235–240.
44. Sun, Q.; Zhang, W.Q.; Xue, L.; Zhang, Z.Z.; Su, T.M. Thermal damage pattern and thresholds of granite. *Environ. Earth Sci.* **2015**, *74*, 2341–2349. [[CrossRef](#)]
45. Somerton, W.H.; Boozer, G.D. A method of measuring thermal diffusivities of rocks at elevated temperatures. *AIChE. J.* **2010**, *7*, 87–90. [[CrossRef](#)]
46. Hartlieb, P.; Toifl, M.; Kuchar, F.; Meisels, R.; Antretter, T. Thermo-physical properties of selected hard rocks and their relation to microwave-assisted comminution. *Miner. Eng.* **2016**, *91*, 34–41. [[CrossRef](#)]
47. Just, J.; Kontny, A. Thermally induced alterations of minerals during measurements of the temperature dependence of magnetic susceptibility: A case study from the hydrothermally altered Soultz-sous-Forêts granite, France. *Int. J. Earth Sci.* **2012**, *101*, 819–839. [[CrossRef](#)]



© 2018 by the authors. Licensee MDPI, Basel, Switzerland. This article is an open access article distributed under the terms and conditions of the Creative Commons Attribution (CC BY) license (<http://creativecommons.org/licenses/by/4.0/>).